IEEE Access
Multidisciplinary | Rapid Review | Open Access Journal

Received September 29, 2019, accepted October 21, 2019, date of publication November 7, 2019,
date of current version November 19, 2019.

Digital Object Identifier 10.1109/ACCESS.2019.2952210

Protection Performance of New Polydimethylsiloxane Packaging Method for Aero-Engine Precision Bearings

YE TIAN[1], JIANGUO CUI[1], FEI YANG[2], XUYAN HOU[2], ZHIHUI SUN[1], JUNYUE TANG[2], AND BO TANG[1]

[1]Light Industry College, Harbin University of Commerce, Harbin 150028, China
[2]College of Mechatronics Engineering, Harbin Institute of Technology, Harbin 150001, China

Corresponding authors: Fei Yang (yangf@hit.edu.cn) and Xuyan Hou (houxuyan@hit.edu.cn)

This work was supported in part by the National Natural Science Foundation of China under Grant 41772387, in part by the Harbin University of Commerce Doctoral Scientific Research Foundation under Grant 2016BS07, and in part by the Youth Innovative Talent Support Program of Harbin University of Commerce under Grant 2016QN067.

ABSTRACT Packaging that is currently used for aero-engine precision bearings faces several issues, such as insufficient cushioning performance, insufficient sealing performance, and poor visibility. Herein, we propose a new method in which the bearings are fully covered with polydimethylsiloxane (PDMS). Samples were prepared for tensile and moisture-permeability tests according to the optimum ratio 10:1 (PDMS: Curing agent) of PDMS provided in the literature. The stress and strain curves of PDMS were then obtained via the tensile test. Additionally, the permeability of a polyethylene/polyamide composite film (the packaging material currently used) and PDMS were compared via a moisture-permeability test. According to the test results, the cushioning coefficient of silicone was 1.9, and the minimum thickness of the pad was 12 mm. Using a finite-element software, the bearing stress of the buffer pad was compared for thicknesses of 7, 12, 17, and 22 mm. The simulation results indicated that the liner with a pad thickness of 12 mm provided the optimal protection and economy. According to the simulation results, the precision bearing is packed in such a manner that it is fully enclosed, and the suitability of the proposed method wherein the PDMS material is used as a cushion pad was verified by simulating a drop test of the product during transportation. When the thickness of the PDMS cushion was 12 mm, the shock acceleration of the bearing was <1100 m/s^2. Thus, the proposed method can successfully protect aero-engine precision bearings.

INDEX TERMS Aero-engine precision bearing, cushion packaging, PDMS, simulation, drop test.

I. INTRODUCTION

Precision bearings are the most important parts of an aero-engine. The high performance and long service life of an aircraft depend on the quality of the bearings. Most researchers focus on the quality of precision bearings when they are used in a machine [1]–[4]. However, the protection of these bearings by packaging during transportation is generally ignored. The traditional packaging method of aero-engine bearings has drawbacks with regard to sealing, buffering, and visibility. A sealed bag cannot prevent moisture from entering a package for a prolonged period; thus, it cannot reduce the adverse effect on transportation. The traditional packaging method allows the production of high-quality bearings; however, the quality of the packaging is low. The defect rate and enterprise operating cost increase significantly. The purpose of this paper is to explore the feasibility of PDMS as an Aero-Engine Precision bearing Packaging. The research results have important reference value to avoid bearing damage during transportation, reduce damage rate and improve the economic benefit of enterprises.

Polydimethylsiloxane (PDMS) is a well-known material used in microelectromechanical systems technology. Its composites can be used in pressure sensors and various energy-harvesting devices [5], [6]. A PDMS sheet was used as a substitute for a Pyrex glass wafer to seal the rear of V-grooved chambers of pressure-sensor chips [7]. The stress–strain curve of the material was obtained via a static compressive

The associate editor coordinating the review of this manuscript and approving it for publication was Chaitanya U. Kshirsagar.

test of polyethylene foam. The dropping impact acceleration of the polyethylene foam buffer system was simulated. The results were analyzed and compared with the drop-test results [8]. To simulate the actual transportation of the product, the effect of low-strength repeated impacts on the cushioning performance of honeycomb paperboard was studied. Additionally, the load–displacement curves and energy-absorption diagrams of the honeycomb paperboard were obtained [9], [10]. An appropriate PDMS packaging improves the stability with regard to superhydrophobic surfaces. In one study, a water-repellent surface was prepared, with a contact angle of 153° and a sliding angle of 1° [11]. Because the mechanical properties of PDMS are closely related to the weight ratio of the pre-polymer to the curing agent, five different ratios—5:1, 7.5:1, 10:1, 12.5:1, and 15:1—were chosen to achieve different Young's moduli of the samples [12], [13]. V-notched samples of SBR were tested under tensile loading, and their rupture displacements were determined. The rupture loads of the tested rubbers were predicted using the averaged strain energy density criterion [14]. Compared with the Young's moduli obtained in other studies, S. Johari found that the two main factors that affect the Young's modulus for PDMS were the baking time and curing temperature; higher temperatures and longer baking times increased the stiffness of the PDMS material [15]. A new constitutive equation for rubber was derived by employing a non-affine molecular chain network model. The deformation behaviors of two-dimensional rubber unit cells containing silica fillers under monotonic and cyclic straining were investigated via a computational simulation [16]. For safety and transparency, PDMS is used to sealing small electrical device, prosthesis manufacture and adhesive. However, few people [17], [18] use PDMS as a transportation package for buffering and universal mechanical products. The shortcomings of the currently used packaging methods were tested and analyzed. A new packaging method for aero-engine bearings using PDMS is proposed herein. According to the mechanical models, the thickness of the cushion liner for PDMS was calculated. The mechanical properties of PDMS were determined via a tensile test. Then, a dropping simulation was performed to compare the effects of different thicknesses of the PDMS padding. To verify the analysis results and the rationality of the packaging method, a dropping simulation test was conducted wherein the package was dropped from different heights.

II. CURRENT PACKAGING DEFECTS

Aero-engine bearings are available in a variety of structures. Additionally, an aircraft has many types of bearings. The various uses of bearing causes different outer envelope sizes. This has led to a general increase in the level of technical requirements. It is difficult to use standard packaging to protect all the bearings. The universality of bearing packaging is quite important.

Bearings must undergo a series of processes, such as handling, transportation, and storage. During each process, the vibration and shock can damage the bearing surface. Moisture can enter the package and cause rust on the surface.

FIGURE 1. Current packaging of bearings.

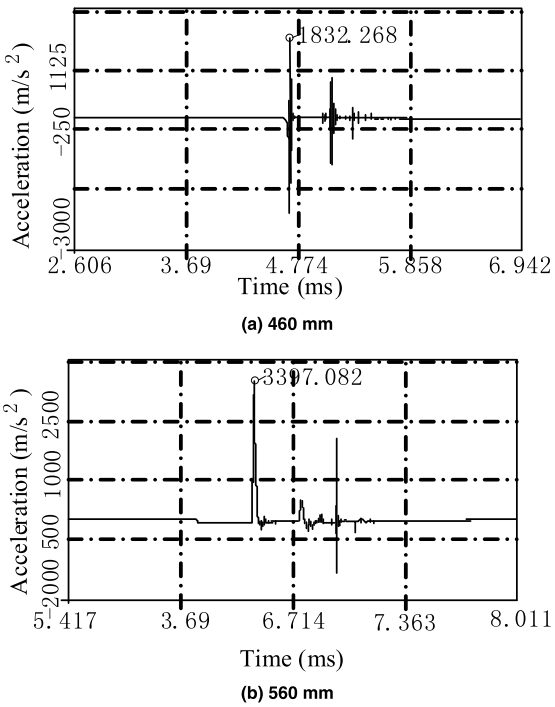

FIGURE 2. Acceleration curves of bearings dropped from heights of (a) 460 mm and (b) 550 mm.

The current packaging of bearings is shown in FIGURE 1. The bearing is wrapped in a plastic bag (made of polyethylene/polyamide (PE/PA)). Then, it is placed in a corrugated cardboard box with a thickness of 7 mm. The plastic bag can protect the bearing from dust and water. However, it cannot provide this protection for a prolonged period. The box can protect the bearing from abrasion; however, it cannot absorb the shock when the package is dropped.

FIGURE 2 shows a comparison of the bearing shock acceleration when the package is dropped from 460 and 560 mm. When the box is dropped from 760 mm, the bearing shock acceleration exceeds the sensor range. The acceleration data are presented in TABLE 1. The average acceleration values for the dropping heights of 460 and 560 mm are 1515.67 and 2598.21 m/s^2, respectively.

TABLE 1. Drop-test data of the current bearing packaging.

Height /m	1st /m·s^{-2}	2nd /m·s^{-2}	3rd /m·s^{-2}	4th /m·s^{-2}	Avg /m·s^{-2}
460	1611.04	1832.26	1432.65	1636.75	1515.67
560	2988.51	2396.23	1611.04	3397.08	2598.21

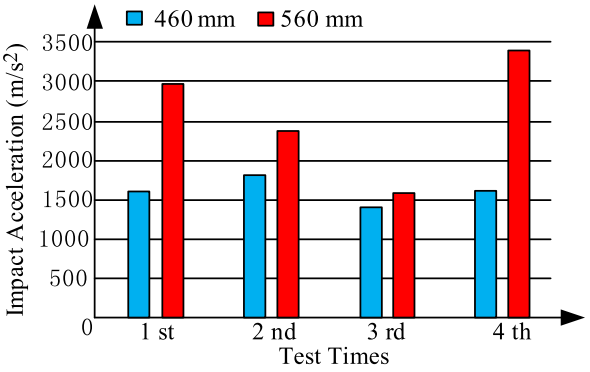

FIGURE 3. Comparison of acceleration of bearings dropped from different heights.

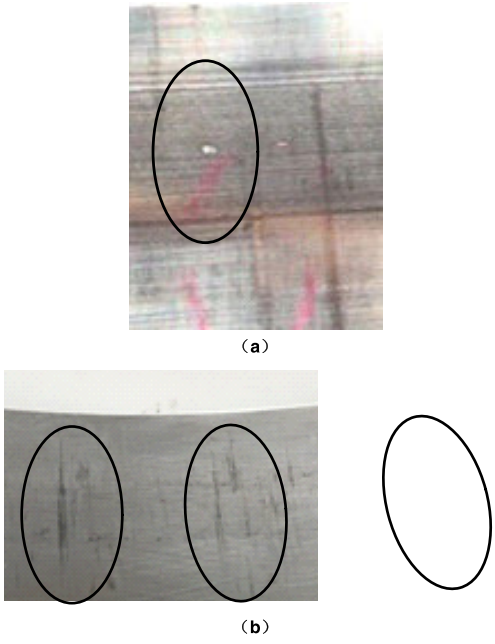

FIGURE 4. Damage on the surface of the inner ring.

The acceleration increases with the dropping height, as shown in FIGURE 3. For a shock value exceeding the permissible value for aviation products, i.e., 110 G, the bearing can be damaged. FIGURE 4 shows the point damages and scratches on the surface of the outer ring. The damage is difficult to observe with the naked eye; a powerful microscope is required.

III. PDMS SEAL PACKAGE AND MATERIAL CHARACTERS

A. IDEA OF PDMS SEAL PACKAGE

The drawbacks of the current packaging methods are the poor anti-seepage capability and buffering. In this paper, we present a new method of aero-engine bearing packaging. The aero-engine bearings are fully covered by PDMS. PDMS is translucent, elastic, and nontoxic. Owing to its elastic and nontoxic properties, PDMS is a suitable material for packaging aero-engine bearings, which require cushioning and protection against rust during transportation. The user can see the bearing directly through the PDMS owing to its hyaline characteristic. After the bearing is removed from the package, the remaining packaging can be recycled. Relative to the current packaging, there are several advantages of PDMS as a bearing packaging. It can be seen from TABLE 2, PDMS have several advantages to be a bearing packaging material relative to current packaging. The initial liquid state is universality for different shape of products.

TABLE 2. Advantages of PDMS as packaging material.

Name	Visibility	Cushioning	Recyclability	Universality
Current packaging	No	No	No	No
PDMS packaging	Yes	Yes	Yes	Yes

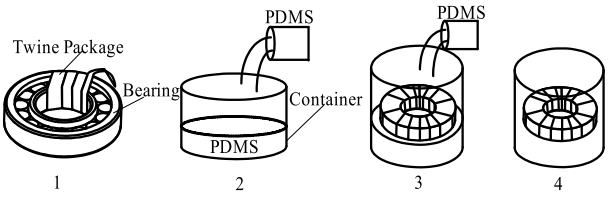

FIGURE 5. PDMS packaging process for the bearing.

The packaging process of aero-engine bearings, which involves four steps, is shown in FIGURE 5. First, to separate the PDMS and the bearing, a flexible PE material is used to cover the bearing. Second, PDMS is poured into a container to form a cushion. After the PDMS solidifies into a cushion, the bearing is placed on the cushion, and PDMS is poured into the container again to fully cover the bearing. The final package is shown in FIGURE 6.

B. TESTS OF PDMS SAMPLES

1) PREPARATION OF PDMS TEST PIECES

PDMS is a nontoxic, hydrophobic, nonflammable, and transparent thermoplastic elastomer. It is widely used in material synthesis and in the industrial field. The performance of PDMS conforms to the technical requirements for the bearing packaging. According to the literature [12], [13], the proportion of the PDMS material, which was composed of dimethyl silicone oil and a curing agent, was 10:1. The PDMS was manufactured by AUSBOND company of US. The mixture was stirred using a machine at 23 °C. After stirring for 30 min, the mixture was injected into a mold, as shown in FIGURE 7, and allowed to remain until it solidified. The mold was designed to shape a test piece in accordance with the ASTM D3183 standard [19]. The thickness of the test piece was 3 mm.

FIGURE 6. Final package of the bearing.

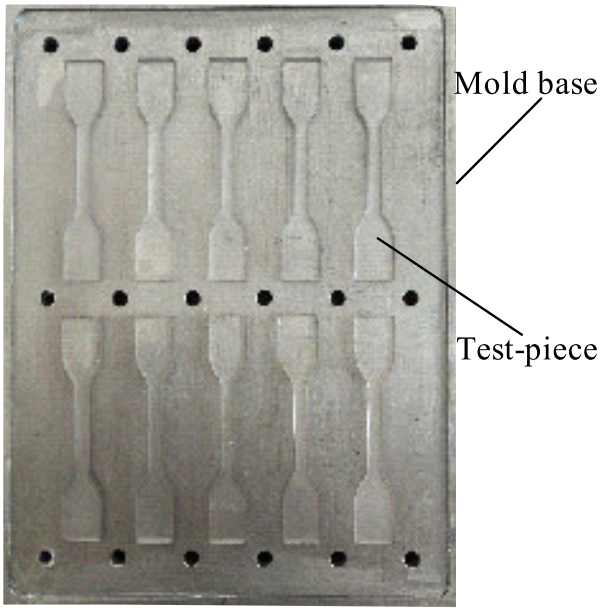

FIGURE 7. Test piece samples of PDMS.

TABLE 3. Properties of MOCON PERMATRAN-W 1/50 G.

Property	Quantity
Area	50 cm^2
Temperature	10-40 ℃
Humidity	35-90 RH
Test range	0.1-100 g/cm^2 day

2) WATER VAPOR TRANSMISSION RATE (WVTR) TEST

The WVTR of the PDMS was tested using a MOCON PERMATRAN-W 1/50 G. It was manufactured by MOCON company of US, and the properties were shown in Table 3.

The relative humidity, temperature, and N_2 pressure were maintained at 75%, 25 °C, and 0.21–0.23 MPa, respectively.

TABLE 4. WVTR.

NO.	PE/PA (g/cm^2 day)	PDMS (g/cm^2 day)
1	2.349	0.08
2	1.006	0.001
3	1.17	0.001
4	1.03	0.001

FIGURE 8. Beginning of tensile test.

TABLE 5. Properties of Zwick.

Property	Quantity
Test speed range	0.0005 to 1000 mm/min
Max tensile force	100 kN
Distance of testing	1050-1370 mm

The WVTRs of PDMS and PE/PA are presented in TABLE 4. As shown, the WVTR of PDMS was lower than that of PE/PA. This is not only because the PDMS was thicker than the PE/PA but also because the PDMS had superior characteristics to the PE/PA.

3) TENSILE TEST

FIGURE 8 shows the beginning of the tensile test of PDMS conducted using a Zwick machine in accordance with the ASTM D412 standard [20]. Zwick was manufactured by ZwickRoell company of Germany, and the properties were shown in Table 5.

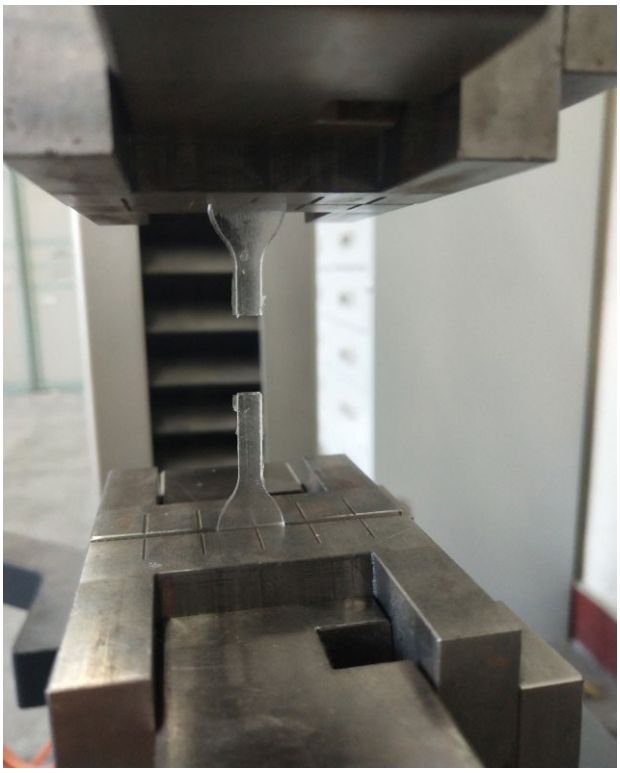

FIGURE 9. End of tensile test.

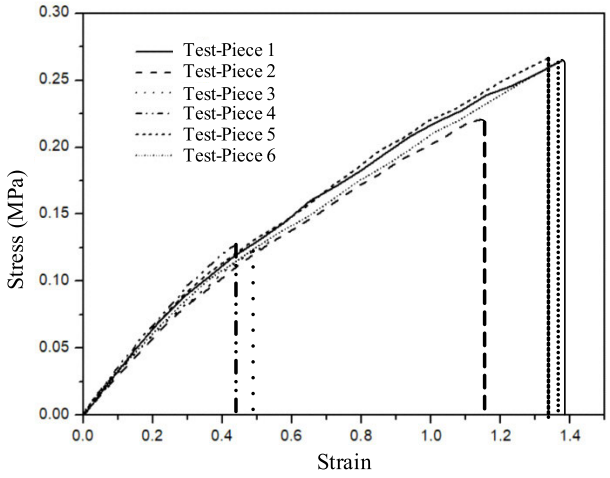

FIGURE 10. Stress–strain curve of PDMS.

The tensile velocity of the jig was maintained at 5 mm/min until the specimen was fractured, as shown in FIGURE 9.

Six tensile-test results are shown in FIGURE 10. All six curves exhibited the same trend. Several curves overlapped, indicating the small error. When the specimen was fractured, the stress–strain curve of PDMS decreased sharply.

C. BUFFER COEFFICIENT AND PAD THICKNESS CALCULATION FOR PDMS

According to the stress–strain curve, the steps for calculating the buffer coefficient are as follows.

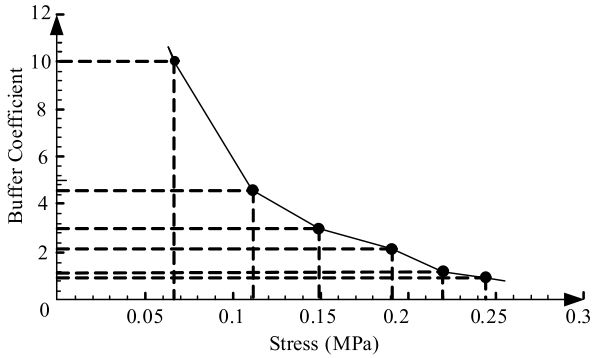

FIGURE 11. Buffer coefficient and stress curve of PDMS.

TABLE 6. Drop test for the criterion of height [21].

Weight (kg)	0-10	10-19	19-28	28-45	45-68
Dropping Height (mm)	760	610	460	310	200

(1) The area under the σ–ε curve is divided into several regions. The junction points are calculated as σ_i on the axis of the stress ($i = 1, 2, 3, \ldots$) and as ε_i on the axis of the strain ($i = 1, 2, 3, \ldots$).

(2) The areas of the regions are as follows:

$$\Delta e_i = \frac{1}{2}(\sigma_i + \sigma_{i-1})(\varepsilon_i - \varepsilon_{i-1}) \tag{1}$$

(3) The formula for calculating the deformation energy caused by the stress σ_i is as follows:

$$e_i = \sum_{j=1}^{i} \Delta e_j. \tag{2}$$

(4) The formula for calculating the buffer coefficient caused by the stress σ_i is as follows:

$$B_i = \frac{\sigma_i}{e_i}. \tag{3}$$

Based on the buffer-coefficient curve of PDMS is shown in FIGURE 11.

The diameters of the outer and inner rings of the aero-engine bearing were 180 and 130 mm, respectively. The weight of the bearing was 2.2 kg. As a general aerospace product criterion, the fragility of the bearing was 110 G, as shown in TABLE 6, and the dropping height of the bearing was 760 mm.

The buffer pad for the PDMS was placed at the bottom of the bearing. Therefore, the contact area between the bearing and the buffer pad was toroidal, the inner and outer diameters of which were identical to those of the bearing.

$$A = \pi R_1^2 - \pi r_1^2 = 0.0122\ \mathrm{m}^2 \tag{4}$$

Here, R_1 represents the outer diameter of the bearing, and r_1 represents the inner diameter of the bearing.

The maximum stress on the buffer pad was

$$\sigma_m = \frac{WG_c}{A} = 0.212\ \mathrm{MPa} \tag{5}$$

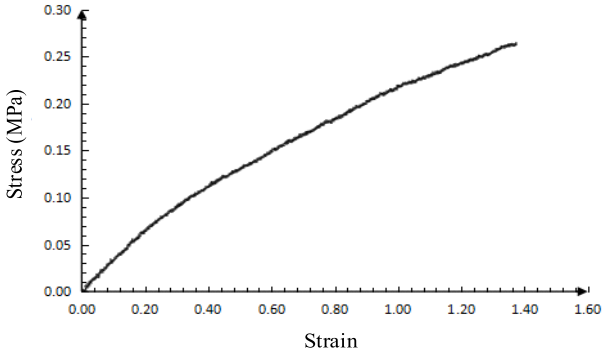

FIGURE 12. Fitting curve of PDMS.

where W represents the weight of the bearing, and G_c represents the fragility of the bearing.

As σ_m was 0.212 MPa on the horizontal axis, the obtained buffer coefficient was 1.9, as shown in Figure 12. Therefore, the thickness of the buffer pad was

$$T = \frac{BH}{G_c} = 12 \text{ mm} \tag{6}$$

where H represents the dropping height.

The minimum thickness of the buffer was 12 mm. If the pad thickness is <12 mm, the fragility exceeds the permissible value, which can cause damage to the bearings.

IV. SIMULATION ANALYSIS

A. MECHANICAL MODEL OF PDMS BUFFER PAD

PDMS silicone is defined as an isotropic hyper-elastic material according to continuum mechanics. The stress energy density is expressed as the sum of the strain deviation energy and the volume strain energy [16], [22]. The formula is as follows:

$$W = f(\bar{I}_1 - 3, \bar{I}_2 - 3) + g(J - 1) \tag{7}$$

The Yeoh model is used not only to describe the mechanics of silicone but also to predict its mechanical behavior, particularly during large-deformation simulations. When the order of the polynomial is three, the formula is as follows:

$$W = \sum_{i=1}^{3} C_{i0}(\bar{I}_1 - 3)^i + \sum_{i=1}^{3} \frac{1}{D_i}(J - 1)^{2i} \tag{8}$$

where W represents the stress energy density, C_{i0} represents the Rivlin coefficient, $\bar{I}_1$ represents the first invariant of the deformation tensor E, D_i is the determination coefficient of deformation, and J represents the volume deformation ratio. We consider the partial derivatives I_1 and I_2 as follows:

$$\frac{\partial W}{\partial I_1} = C_{10} + 2C_{20}(I_1 - 3) + 3C_{30}(I_1 - 3)^2 \tag{9}$$

$$\frac{\partial W}{\partial I_2} = 0 \tag{10}$$

Then, the stress is expressed as follows:

$$\sigma = 2[(1+\varepsilon) - (1+\varepsilon)^{-2}][C_{10} + 2C_{20}(I_1 - 3) + 3C_{30}(I_1 - 3)^2] \tag{11}$$

TABLE 7. Parameters of bearings and silica cushion.

Name	Density of bearing	Young's of bearing	Poisson ratio of bearing	Density of silica	Friction coefficient of silica and steel
Parameters	7800 kg/m^3	210 GPa	0.3	1030 kg/m^3	0.3

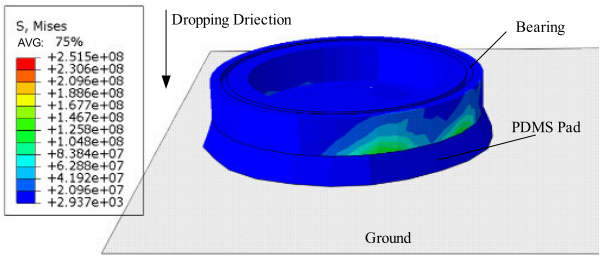

FIGURE 13. Dropping simulation.

The formula for obtaining C_{10}, C_{20}, and C_{30} is as follows:

$$\sigma = 2[(1+\varepsilon) - (1+\varepsilon)^{-2}]\{C_{10} + 2C_{20}[(1+\varepsilon)^2 + 2(1+\varepsilon)^{-1} - 3] + 3C_{30}[(1+\varepsilon)^2 + 2(1+\varepsilon)^{-1} - 3]^2\} \tag{12}$$

According to the tensile-test data, the Rivlin coefficients were obtained as follows: $C_{10} = 771.13 \times 10^{-3}$,$C_{20} = -48.01 \times 10^{-3}$, and $C_{30} = 10.29 \times 10^{-3}$. C_{10} represents the initial shear modulus. C_{20} was negative because the material was softened with moderate deformation. The positive value of C_{30} indicates that the material became hard after large deformation.

According to (12), the fitting curve is shown in FIGURE 12. The formula was used to describe the mechanical behavior of PDMS in the finite-element analysis software.

B. DROP-TEST SIMULATION

The fitting-curve data were input into the ABAQUS software to describe the characteristics of the PDMS buffer pad. A drop test was simulated in ABAQUS to compare the performance for pads of different thicknesses. The parameters of the bearing and silica are presented in Table 7.

According to the formula (6), the minimum thickness of buffer pad is 12 mm. Therefore, 12 mm thickness of PDMS is taken as a standard value. The buffer pad cannot give a protection to bearing if thickness less than 12 mm. On the contrary, the bearing is protected when pad thickness is more than 12 mm. In order to obtain obvious simulation result, choose 5 mm as the thickness difference. In finite element analysis software environment, four thicknesses, such as 7, 12, 17, and 22mm were simulated. Since the current package thickness of corrugated board is 7 mm, 7 mm is set to the minimum value. As shown in FIGURE 13, the bearing was fixed on the buffer pad and fell to the ground, as in the real test.

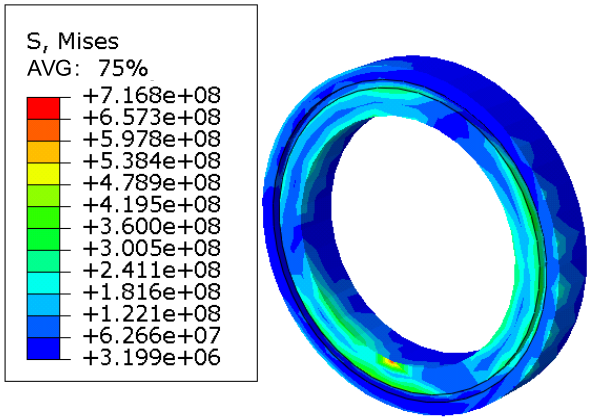

FIGURE 14. Stress on the bearing with the 7-mm-thick pad.

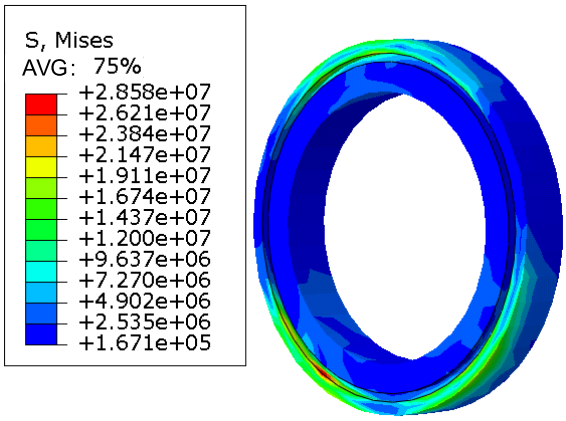

FIGURE 15. Stress on the bearing with the 12-mm-thick pad.

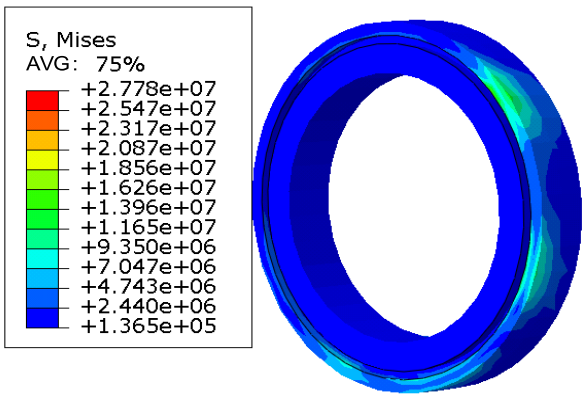

FIGURE 16. Stress on the bearing with the 17-mm-thick pad.

As shown in FIGURES 14–17, after the dropping, the stress on the bearing was distributed on the inner ring at the bottom. FIGURE 14 shows that the stress on the bearing was 717 MPa when the thickness of the pad was 7 mm. The maximum value of the stress occurred at the bottom of the inner ring, which was in contact with the buffer pad. FIGURE 15 shows that the stress on the bearing was 286 MPa when the thickness of the pad was 12 mm. The

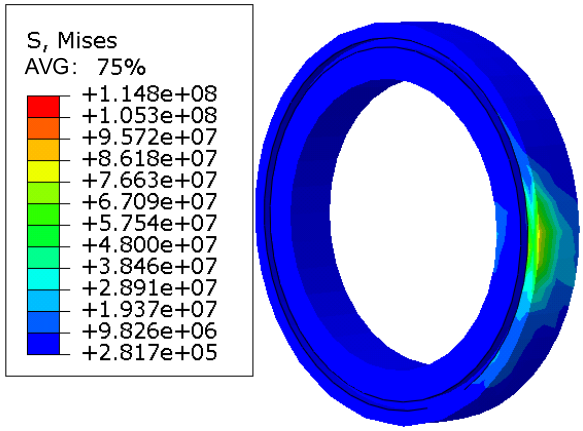

FIGURE 17. Stress on the bearing with the 22-mm-thick pad.

stress-distribution area in this case was smaller than that for the 7-mm thickness. However, the maximum stress occurred at the bottom of the outer ring, which was in contact with the buffer pad. FIGURE 16 shows that the stress on the bearing was 278 MPa when the thickness of the pad was 17 mm. The stress-distribution area in this case was smaller on the outer ring compared with the case where the pad thickness was 12 mm. The lowest stress among the four simulations was observed for the 22-mm-thick pad. It was 115 MPa when the bearing and pad were dropped on the ground. Furthermore, the stress-distribution area in this case was the smallest among the four simulations, as shown in FIGURE 17. Analyzing FIGURES 14–17 reveals that with the increasing thickness of the PDMS buffer pad, the stress on the bearing decreased, and the distribution area decreased from the inner ring to the outer ring.

The annealed yield strength of the bearing steel ranged from 353 to 382 MPa. The stress on the bearing when it was dropped with the 7-mm-thick PDMS pad exceeded the permissible stress of 353 MPa. Therefore, the bearing was damaged when the thickness of the pad was 7 mm, which was not the case with the other three pads.

FIGURE 18 shows the stress curve obtained from the bearing simulation wherein the bearing with four different buffer pads was dropped from the same height. A thicker PDMS pad led to a lower stress generated on the bearing. Considering the product cost, a PDMS buffer pad thickness of 12 mm is sufficient to prevent damage caused by dropping.

V. TESTS AND RESULTS

Characteristics of transportation, such as the type of vehicle employed, pavement quality of the road, driving status, and means of handling, are key factors that impact the bearing. Collisions during transportation damage the contact surface between the rolling element and rings, adversely affecting the bearing quality.

To examine the impact acceleration of the bearing as a criterion, a series of tests were conducted to simulate the free drop that occurs during transportation. FIGURE 19 shows

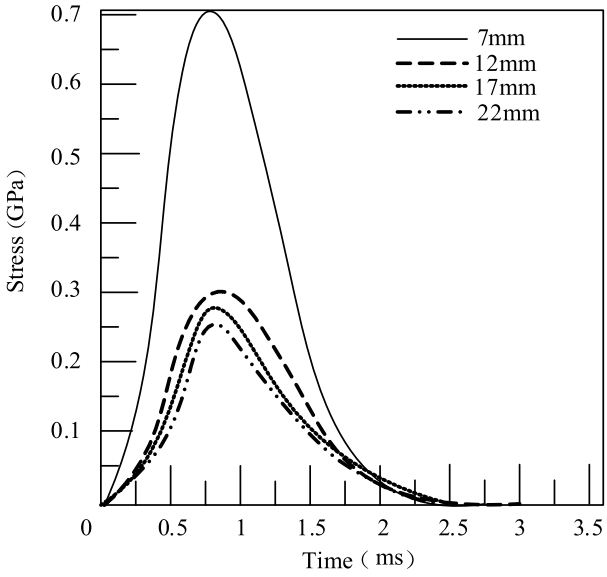

FIGURE 18. Stress on the bearing for different thicknesses of the buffer pad.

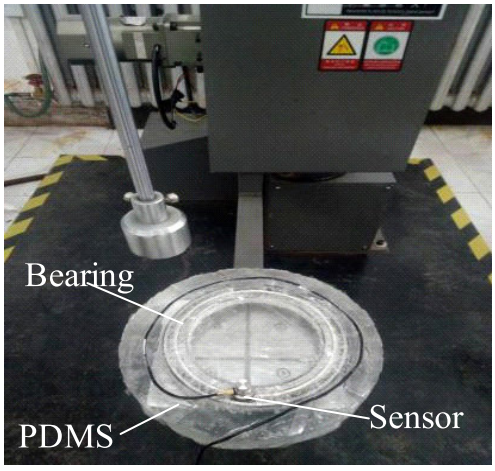

FIGURE 19. Sensor and package.

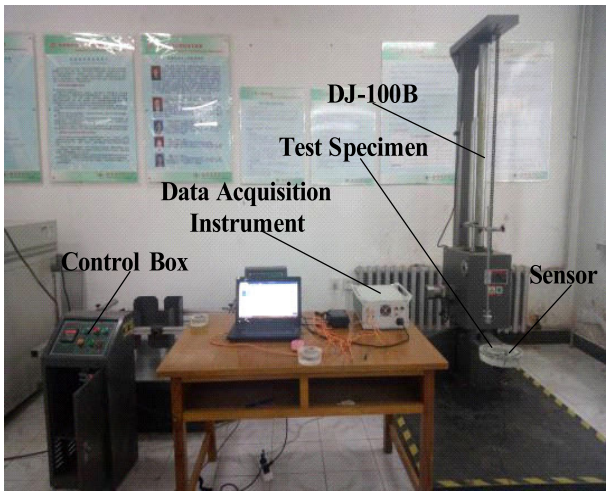

FIGURE 20. Drop-test system.

TABLE 8. Properties of dropper.

Property	Quantity
Dropping height	300-2000 mm
Test object weight	0-100 kg
Volume of test object	1000 mm *800 mm *1000mm
Power	0.85 kW

TABLE 9. Properties of data-acquisition instrument.

Property	Quantity
Acceleration range	10-3000 m/s^2
Pulse duration	0.1-100 ms
Passageway	8

that the bearing was fully covered by PDMS, and an opening was formed at the top of the package to fix a sensor on the bearing. Then, the test specimen was placed on a single-arm dropper.

As shown in FIGURE 20, the test system was composed of the acceleration sensor, the DJ-100B single-arm dropper, a control box, and a data-acquisition instrument.

DJ-100B was manufactured by WuZhong TEST company of China, and the properties were shown in Table 8.

Data-acquisition instrument was manufactured by DongLing TEST company of China, and the properties were shown in Table 9.

The test processes is shown in FIGURE 21. The single-arm was stopped at the required dropping height. Then, it swung rapidly and test specimen dropped to the ground directly as shown in FIGURE 21 (a). when the test is parked on the ground, the impact acceleration is obtained by the data-acquisition instrument, as shown in FIGURE 21 (b).

The preparation and steps of the drop test were based on ASTM D5276-98 [23], [24]. The packaged bearings was dropped four times from heights of 460, 560, and 760 mm. The standard dropping height in ASTM D5276-98 is 760 mm. The other two heights were the distances between the ground and the hands of the people who dropped the package. The thickness of the PDMS was 12 mm. FIGURE 22 depicts the impact of the acceleration on the time domain when the package was dropped from a height of 760 mm. The first acceleration peak occurred when the package hit the ground. The other peaks were caused by the rebounding of the package.

The dropping test data are shown in TABLE 10. When dropped from 460 mm, the maximum acceleration of the bearing is 613.863 m/s^2, and the minimum is 510.481 m/s^2. When dropping height increased from 460 mm to 560 mm, the maximum acceleration of the bearing is 680.811 m/s^2, and the minimum is 646.546 m/s^2. When dropping height is

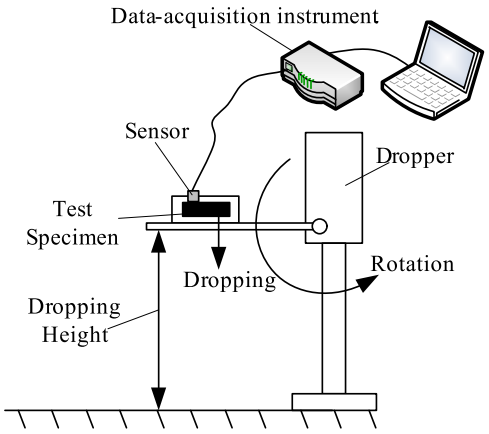

(a) Beginning of test

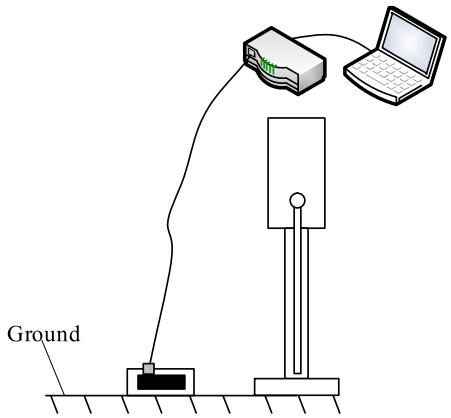

(b) End of test

FIGURE 21. Test process.

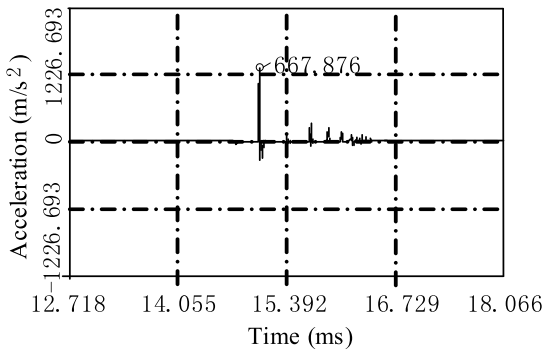

FIGURE 22. Shock acceleration curve with the cushioning package.

760mm, the maximum acceleration of the bearing is 833.833 m/s^2, the minimum is 785.283 m/s^2. The average data are lower than 1100 m/s^2 (110 G). The results indicate that the PDMS pad absorbed impact caused by dropping. The impact acceleration cannot damage the bearing. The bearing is protected well in the PDMS package.

FIGURE 23 shows a comparison between PDMS packaging and traditional packaging dropped from the same height.

TABLE 10. Drop-test data for bearing package with PDMS cushion.

Height /mm	1st /m·s^{-2}	2nd /m·s^{-2}	3rd /m·s^{-2}	4th /m·s^{-2}	Avg /m·s^{-2}
460	510.481	578.892	613.863	517.113	555.087
560	667.876	646.546	651.677	680.811	661.728
760	785.283	833.883	793.697	830.949	810.953

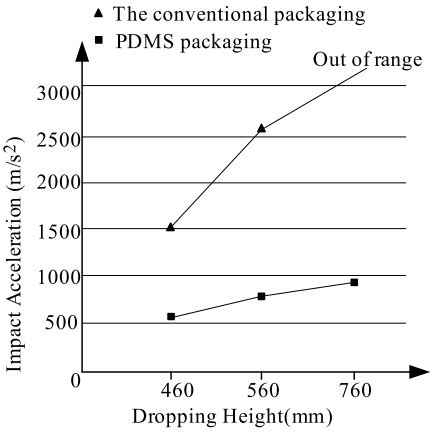

FIGURE 23. Comparison of the acceleration between the prevalent packaging and the PDMS packaging dropped from the same height.

The results show that as the drop height increases, the acceleration of the bearing increases. FIGURE 23 shows, the acceleration of traditional package exceeds the range of the sensor when it drops from 760 mm. The results show that corrugated cardboard can not reduce the drop impact. High impact acceleration can cause bearing damage. It is indicate that the corrugated cardboard cannot reduce the dropping impact. High impact acceleration can cause bearing damage. The average acceleration of the bearing package fully covered by PDMS was lower than that of the current packaging in the FIGURE 23. It is indicate that PDMS pad can absorb impact acceleration for the softness and elastic characteristics. PDMS can weaken impact acceleration when it transmit from the bottom of package. Therefore, the PDMS package shows better buffer performance.

VI. CONCLUSION

According to a defect analysis of the current packaging of aero-engine bearings, a new method in which the bearing is fully covered with PDMS is proposed. The mechanical parameters and WVTR of PDMS reported in the literature were verified via tests. Additionally, the minimum thickness of the PDMS buffer pad was calculated, and the four pads were simulated using a finite-element software. To verify the analysis, the impact of the acceleration of the bearing was examined in drop tests.

(1) Owing to its buffering performance and waterproof and transparent properties, PDMS is effective for fully covering aero-engine bearings.
(2) According to the tensile-test data for PDMS and the theoretical analysis, 12 mm is the minimum thickness of the buffer pad for preventing damage due to dropping.
(3) The cost and buffering performance of the 12-mm-thick pad are superior to those of the other three pads.
(4) For impact accelerations of bearings lower than 110 G, a drop test can be used to verify the packaging method and analysis.

REFERENCES

[1] M. M. Tahir, A. Q. Khan, N. Iqbal, A. Hussain, and S. Badshah, "Enhancing fault classification accuracy of ball bearing using central tendency based time domain features," *IEEE Access*, vol. 5, pp. 72–83, 2016.
[2] F. Xu, X. Song, K.-L. Tsui, F. Yang, and Z. Huang, "Bearing performance degradation assessment based on ensemble empirical mode decomposition and affinity propagation clustering," *IEEE Access*, vol. 7, pp. 54623–54637, 2019.
[3] B. Yao, P. Zhen, L. Wu, and Y. Guan, "Rolling element bearing fault diagnosis using improved manifold learning," *IEEE Access*, vol. 5, pp. 6027–6035, 2017.
[4] Z. Huo, Y. Zhang, P. Francq, L. Shu, and J. Huang, "Incipient fault diagnosis of roller bearing using optimized wavelet transform based multi-speed vibration signatures," *IEEE Access*, vol. 5, pp. 19442–19456, 2018.
[5] Y. Liu, Y. Wei, and P. Chen, "Characterization of mechanical properties of two-dimensional materials mounted on soft substrate," *Int. J. Mech. Sci.*, vol. 151, pp. 214–221, Feb. 2019.
[6] V. Kedambaimoole, V. Shirhatti, N. Neella, P. Ray, K. Rajanna, and M. M. Nayak, "PDMS encapsulated graphene-nickel composite film as flexible tactile sensor," in *Proc. IEEE SENSORS*, Glasgow, U.K., Oct./Nov. 2017, pp. 1–3.
[7] H.-H. Wang, P.-C. Yang, W.-H. Liao, and L.-J. Yang, "A new packaging method for pressure sensors by PDMS MEMS technology," in *Proc. NEMS*, Zhuhai, China, Jan. 2006, pp. 47–51.
[8] Z. Shen, D. Chen, and J. J. Luo, "Simulation analysis of drop impact overload of polyethylene foam cushioning system," *Packag. Eng.*, vol. 37, no. 19, pp. 128–132, Feb. 2016.
[9] Z. W. Wang, L. J. Wang, and C. Y. Xu, "Influence of many low strength impact on the cushioning properties of the honeycomb paperboard," *Chin. J. Appl. Mech.*, vol. 32, no. 3, pp. 31–35, May 2015.
[10] C. Gontier, A. Bouchou, and C. Vinot, "A mechanical model for the computation of phenolic foams in compression," *Int. J. Mech. Sci.*, vol. 43, no. 10, pp. 2371–2384, Oct. 2001.
[11] W. Tong, D. Xiong, T. Tian, and Y. Liu, "Superhydrophobic surface on aeronautical materials via the deposition of nanoparticles and a PDMS seal," *Appl. Phys. A, Solids Surf.*, vol. 125, no. 3, p. 177, Oct. 2019.
[12] M. L. Fitzgerald, S. Tsai, L. M. Bellan, R. Sappington, Y. Xu, and D. Li, "The relationship between the Young's modulus and dry etching rate of polydimethylsiloxane (PDMS)," *Biomed. Microdevices*, vol. 21, no. 1, p. 26, Mar. 2019.
[13] D. Armani, C. Liu, and N. Aluru, "Re-configurable fluid circuits by PDMS elastomer micromachining," in *IEEE Int. MEMS Conf. Tech. Dig.*, Orlando, FL, USA, Jan. 1999, pp. 222–227.
[14] M. Heydari-Meybodi, M. R. Ayatollahi, and F. Berto, "Rupture analysis of rubber in the presence of a sharp V-shape notch under pure mode-I loading," *Int. J. Mech. Sci.*, vols. 146–147, no. 1, pp. 405–415, Oct. 2018.
[15] S. Johari, H. Fazmir, A. F. M. Anuar, M. Z. Zainol, V. Nock, and W. Wang, "PDMS Young's modulus calibration for micropillar force sensor application," in *Proc. IEEE RSM*, Kuala Terengganu, Malaysia, Aug. 2015, pp. 1–4.
[16] Y. Tomita, S. Nakata, T. Honma, and K. Yashiro, "Deformation behavior of silica-filled rubber with coupling agents under monotonic and cyclic straining," *Int. J. Mech. Sci.*, vol. 86, no. 3, pp. 7–17, Sep. 2014.
[17] Z.-Y. Zhang, Y. Tian, W. Liu, H. Zhi, Z.-H. Sun, M.-M. Chen, and P.-P. Yuan, "Cushioning property of aviation bearing PDMS cushion package pad," *Packag. Eng.*, vol. 40, no. 1, pp. 75–79, Feb. 2019.
[18] S. Bin *et al.*, "Improvements on finished products packing of large taper roller bearing," *J. Anyang Inst. Technol.*, vol. 1, no. 6, pp. 16–19, Nov. 2018.
[19] R. Brown, *Physical Testing of Rubbers*. Berlin, Germany: Springer, 2006.
[20] *Standard Test Methods for Vulcanized Rubber and Thermoplastic Elastomers—Tension*, Standard ASTM D412-6, ASTM, 2016.
[21] D. Gao and H. L. Ji, *Packaging Dynamics*. Beijing, China: China Light Industry Press, 2009, pp. 105–110.
[22] H. Wang, "Application of hyper-elastic constitutive models on rubbers in tyre analysis," M.S. thesis, Harbin Inst. Technol., Harbin, China, 2008.
[23] T. Y. Tee, H. S. Ng, C. T. Lim, E. Pek, and Z. Zhong, "Impact life prediction modeling of TFBGA packages under board level drop test," *Microelectron. Rel.*, vol. 44, no. 7, pp. 1131–1142, Jul. 2004.
[24] C. Y. Zhou, T. X. Yu, and R. S. W. Lee, "Drop/impact tests and analysis of typical portable electronic devices," *Int. J. Mech. Sci.*, vol. 50, no. 5, pp. 905–917, May 2008.